

Measurements of the vector boson production with the ATLAS detector

A. Lapertosa^{1,2,*}, on behalf of the ATLAS Collaboration

¹Università degli Studi di Genova

²INFN Sezione di Genova

Abstract. Measurements of the Drell-Yan production of W and Z bosons at the LHC provide a benchmark of our understanding of perturbative QCD and probe the proton structure in a unique way. The ATLAS collaboration has performed new high precision measurements at a center-of-mass energy of 7 TeV. The measurements are performed for W^+ , W^- and Z bosons integrated and as a function of the boson or lepton rapidity and the Z mass. Unprecedented precision is reached and strong constraints on Parton Distribution Functions, in particular the strange density are found. Z boson cross sections are also measured at center-of-mass energies of 8 TeV and 13 TeV, and cross-section ratios to the top-quark pair production have been derived. This ratio measurement leads to a cancellation of systematic effects and allows for a high precision comparison to the theory predictions. The production of jets in association with vector bosons is a further important process to study perturbative QCD in a multi-scale environment. The ATLAS collaboration has performed new measurements of Z boson plus jets cross sections, differential in several kinematic variables, in proton-proton collision data taken at a center-of-mass energy of 13 TeV. The measurements are compared to state-of-the-art theory predictions. They are sensitive to higher-order pQCD effects, probe flavour and mass schemes and can be used to constrain the proton structure. In addition, a new measurement of the splitting scales of the k_t jet-clustering algorithm for final states containing a Z boson candidate at a center-of-mass energy of 8 TeV is presented.

1 Introduction

The production of W and Z bosons via the Drell-Yan process is widely studied at the LHC experiments with proton-proton collision, including the ATLAS experiment [1]. Those processes have a clear signature (especially in the lepton decay channels: $Z \rightarrow ll$ and $W \rightarrow lv$) and are characterized by small background contamination. Due to the high production cross section, it is possible to collect large statistics samples of events containing vector bosons.

W and Z boson events, in turn, are common backgrounds in Standard Model measurements, including Higgs boson measurements, and in new physics searches. As a consequence, an improved description of the vector boson production has a positive impact in many ATLAS physics analyses.

Nevertheless, studying in details the production of vector bosons is useful to test the Standard Model accuracy and extract its parameters. It is possible to probe the proton structure, constraining

*e-mail: alessandro.lapertosa@cern.ch

Parton Distribution Functions (PDFs), and to test the perturbative QCD theory, comparing experimental results to state-of-the-art predictions.

In this review, a selection of seven of the most recent ATLAS results on vector boson physics will be presented: W and Z boson production cross section at 7 TeV [2] and 13 TeV [3]; ratio of $t\bar{t}$ over Z boson production cross section at 7, 8 and 13 TeV [4]; Z +jets production cross section at 13 TeV [5]; triple differential Z boson cross section at 8 TeV [6]; angular coefficients of Z boson leptons [7] and splitting scales of anti- k_t algorithm clustered jets [8], both measured with 8 TeV data.

2 W and Z boson cross section at 7 TeV

Several high precision vector boson cross section measurements have been performed on 4.6 fb⁻¹ 7 TeV data, both inclusive and differential. Very good agreement is found between the ATLAS results and the Standard Model in terms of lepton universality, with the measurement of the $W \rightarrow e\nu/W \rightarrow \mu\nu$ ratio and the $Z \rightarrow ee/Z \rightarrow \mu\mu$ ratio, both found to be compatible with unity (see Fig.1).

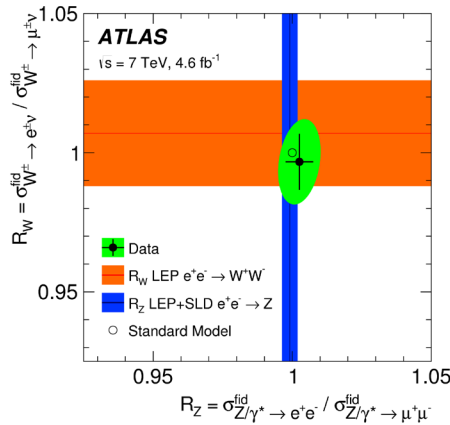


Figure 1. Measurement of the electron-to-muon cross-section ratios for the W and Z bosons. The green shaded ellipse represents the 68% CL for the correlated measurement of W and Z ratios, while the black error bars give the one-dimensional standard deviation. The orange and blue shaded bands represent the combination of the ratios as measured at the LEP and SLAC e^+e^- colliders. The SM expectation is indicated with an open circle. Taken from Ref. [2].

The measurement of the $W \rightarrow l\nu/Z \rightarrow ll$ ratio is sensitive to the strangeness content of the proton. The experimental precision reached is comparable and sometimes better than the one on theoretical predictions. The ATLAS result is compared with predictions obtained adopting different PDFs; in all cases, the predicted cross section ratio values are higher than those measured in data (see Fig. 2), clearly pointing out the need for improvements in the description of the proton structure.

The W boson charge asymmetry A_l , measured as a function of the pseudorapidity of the lepton $|\eta_l|$, defined as:

$$A_l = \frac{d\sigma_{W^+}/d|\eta_l| - d\sigma_{W^-}/d|\eta_l|}{d\sigma_{W^+}/d|\eta_l| + d\sigma_{W^-}/d|\eta_l|}, \quad (1)$$

is found to be in good agreement with the predictions (see Fig. 3), with an accuracy better than 1% across the whole range considered ($|\eta_l| < 2.5$).

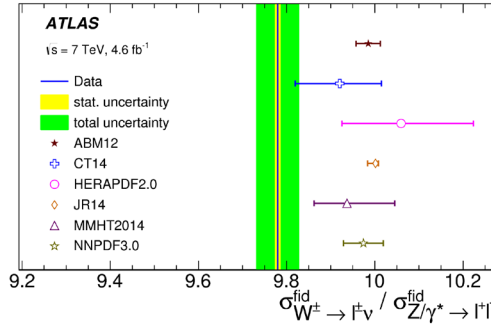


Figure 2. Fiducial cross sections times leptonic branching ratios of the $W \rightarrow lv/Z \rightarrow ll$ ratio. The data (solid blue line) are shown with the statistical (yellow band) and the total uncertainties (green band). The uncertainties of the theoretical calculations correspond to the PDF uncertainties only. Taken from Ref. [2].

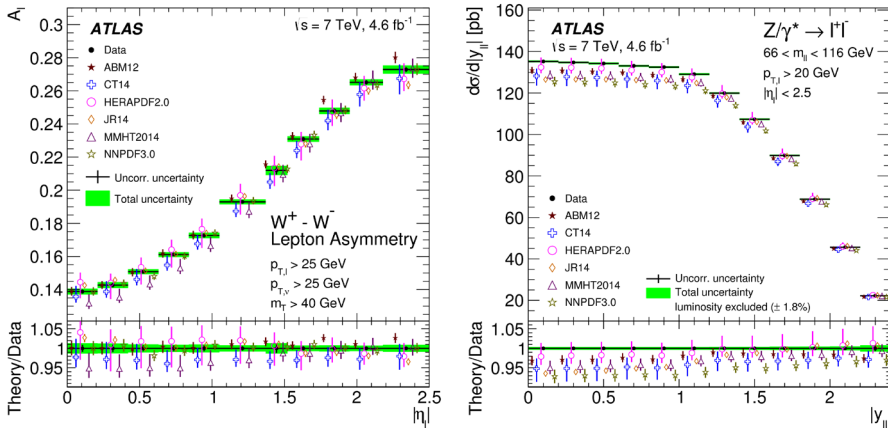


Figure 3. Left: lepton charge asymmetry A_l production as a function of the lepton pseudorapidity. Right: Z boson differential cross-section measurement as a function of the leptons rapidity $|y_{ll}|$. Predictions computed at NNLO QCD with NLO EW corrections using various PDF sets (open symbols) are compared to the data (full points). The ratio of theoretical predictions to the data is also shown. The predictions are displaced within each bin for better visibility. The theory uncertainty corresponds to the quadratic sum of the PDF uncertainty and the statistical uncertainty of the calculation. Taken from Ref. [2].

The Z boson production cross section measured as a function of the leptons rapidity $|y_{ll}|$ is found to be in agreement with predictions for values of $|y_{ll}| > 1$, while for $|y_{ll}| < 1$ the predictions are underestimating the data results (see Fig. 3). This discrepancy can be interpreted as enhanced PDF strangeness content.

Therefore, the results have been used to further constrain the proton PDF: with a profile fit, the new version of the ATLAS based PDF set has been derived, namely *ATLAS-epWZ16*. The new PDF

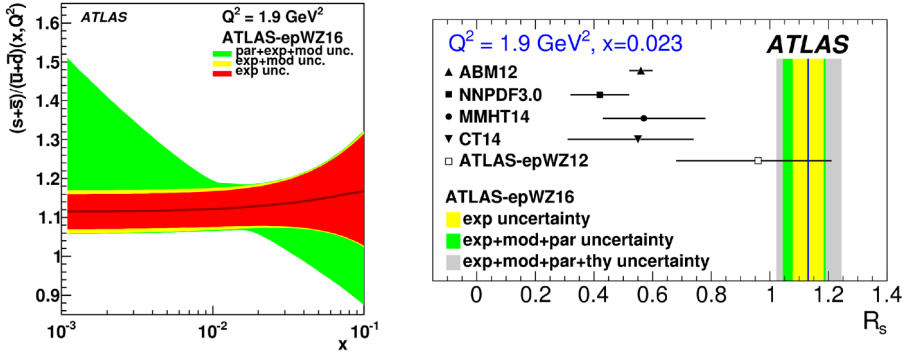


Figure 4. Left: R_s ratio of the PDFs from the present *ATLAS-epWZ16* determination shown in the region of maximum sensitivity of the ATLAS data, $10^{-3} < x < 10^{-1}$. Uncertainty bands represent the experimental (exp), model (mod) and parameterization (par) components in red, yellow and green, respectively. Right: R_s in the region of ATLAS best sensitivity, $Q^2 = 1.9 \text{ GeV}^2$ and $x = 0.023$. Bands: present result and its uncertainty contributions from experimental data, QCD fit, and theoretical uncertainties; Closed symbols with horizontal error bars: predictions from different NNLO PDF sets; Open square: previous ATLAS results. Taken from Ref. [2].

shows unsuppressed strangeness as a function of *Bjorken-x*; in particular, the variable R_s , built as:

$$R_s = \frac{s + \bar{s}}{\bar{u} + d}, \quad (2)$$

is found to be higher than unity in the x range considered ($10^{-3} < x < 10^{-1}$), with larger model uncertainties in the high and low x regions (see Fig. 4). The ATLAS data have the best sensitivity in the region with $Q^2 = 1.9 \text{ GeV}^2$ and $x = 0.023$, where the R_s is measured to be 1.13 ± 0.05 (exp) ± 0.02 (mod) $^{+0.01}_{-0.06}$ (par). With this high precision measurements, ATLAS is definitely accessing the proton structure.

3 W and Z boson cross section at 13 TeV

The W^+ , W^- , W^\pm and Z boson production cross sections have been measured separately in the lepton decay channels with 81 pb^{-1} 13 TeV data, within the fiducial region defined by the detector acceptance. The ATLAS results are compared to theoretical predictions obtained with different PDFs, showing good agreement with many of them. The precision obtained is of the order of 2% on W boson and 1% on Z boson cross section, excluding the 2.1% uncertainty due to the luminosity determination (see Fig. 5).

The cross section ratios benefit from significant cancellation of experimental uncertainties, resulting in higher constraining power. The W^+/W^- ratio measured by ATLAS is found to be systematically lower than the predictions, showing better agreement with the CT14 and MMHT14 PDFs. The W/Z ratio is found to be compatible with the different predictions, within the uncertainty. Both results are shown in Fig. 6.

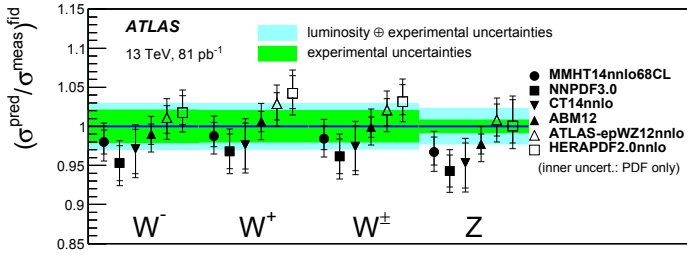


Figure 5. Ratio of the predicted to measured fiducial cross section for the combined electron and muon channels using various PDFs. The inner (outer) band corresponds to the experimental uncertainty without (with) the luminosity uncertainty. The inner error bar of the predictions represents the PDF uncertainty while the outer error bar includes the sum in quadrature of all other systematic uncertainties. Taken from Ref. [3].

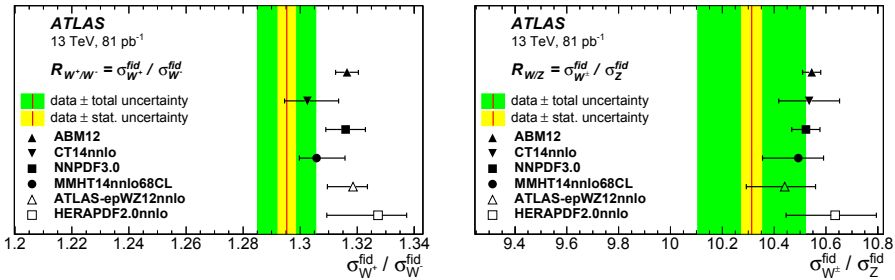


Figure 6. Ratios (red line) of W^+ to W^- boson (left) and W to Z boson (right) combined production cross sections in the fiducial region compared to predictions based on different PDF sets. The inner (yellow) shaded band corresponds to the statistical uncertainty while the outer (green) band shows statistical and systematic uncertainties added in quadrature. The theory predictions are given with only the corresponding PDF uncertainties shown as error bars. Taken from Ref. [3].

4 $t\bar{t}$ over Z boson cross section at 7, 8 and 13 TeV

The $t\bar{t}/Z$ cross section ratio has been measured at 7, 8 and 13 TeV: results are given directly for each considered \sqrt{s} and also as double ratios of the two processes at different \sqrt{s} . The results are corrected to a common phase space and, furthermore, the systematic uncertainties are properly correlated among measurements. The cross section ratio $R_{t\bar{t}/Z}$ is defined as:

$$R_{t\bar{t}/Z} = \frac{\sigma_{t\bar{t}}}{0.5(\sigma_{Z \rightarrow ee} + \sigma_{Z \rightarrow \mu\mu})}, \quad (3)$$

where $\sigma_{Z \rightarrow ee}$ and $\sigma_{Z \rightarrow \mu\mu}$ are the Z boson cross section measured in the electron and the muon channel, respectively.

The results are compared to calculations performed at next-to-next-to-leading-order accuracy using recent PDF sets. The final results uncertainty is further reduced thanks to the cancellation of systematic uncertainties in the ratios, with the data results being more precise than predictions, especially in the 7 and 8 TeV cases (see Fig. 7).

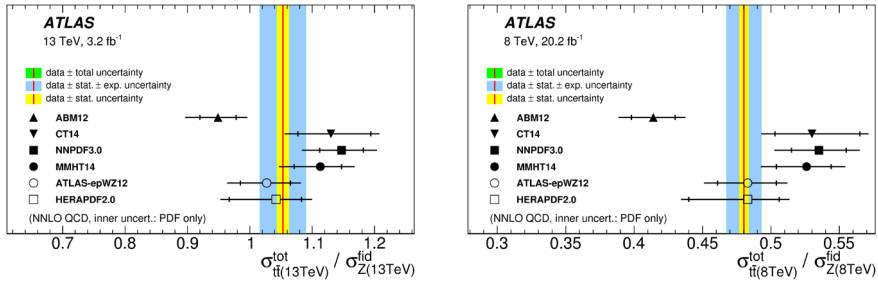


Figure 7. The $t\bar{t}/Z$ cross section ratio for $\sqrt{s} = 7$ TeV (left) and 8 TeV (right): results are compared to predictions based on different PDF sets. The inner shaded band corresponds to the statistical uncertainty, the middle band to the statistical and experimental systematic uncertainties added in quadrature, while the outer band shows the total uncertainty, including the luminosity uncertainty which almost entirely cancel in these ratios. The theory predictions are given with the corresponding PDF uncertainties shown as inner bars while the outer bars include all other uncertainties added in quadrature. Taken from Ref. [4].

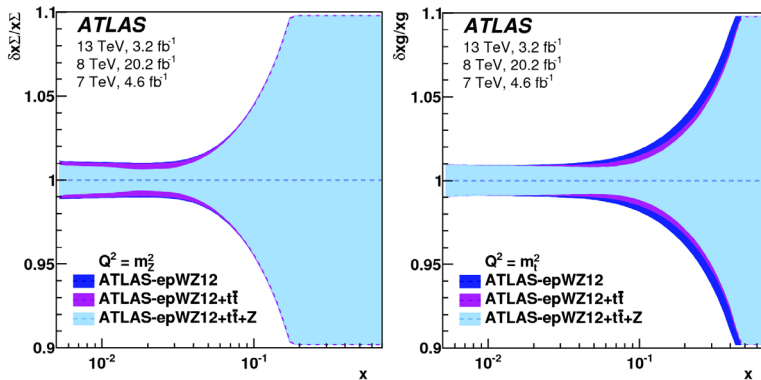


Figure 8. Impact of the ATLAS Z boson and $t\bar{t}$ cross-section data on the determination of PDFs. The bands represent the uncertainty for the *ATLAS-epWZ12* PDF set and the uncertainty of the profiled *ATLAS-epWZ12* PDF set using Z boson and $t\bar{t}$ data as a function of x for the total light-quark-sea distribution (left) for the gluon density (right). The plots also show the impact of only including the ATLAS $t\bar{t}$ data set. Taken from Ref. [4].

The six measured cross sections ($t\bar{t}$ and Z cross sections at 7, 8 and 13 TeV) are used together within a profile fit to further constrain the *ATLAS-epWZ12* PDF: significant reductions of the uncertainties are obtained for the gluon distribution function for x values near 0.1 and for the light-quark sea for $x < 0.02$ (see Fig. 8).

5 Z +jets production cross section at 13 TeV

The measurements of the production cross section of a Z boson in association with jets is performed on 3.16 fb^{-1} 13 TeV data. Inclusive and differential cross sections are measured for events containing a Z boson decaying to electrons or muons and produced in association with up to seven jets with $p_T > 30 \text{ GeV}$ and $|\eta| < 2.5$. The data results are compared to different order predictions: in general,

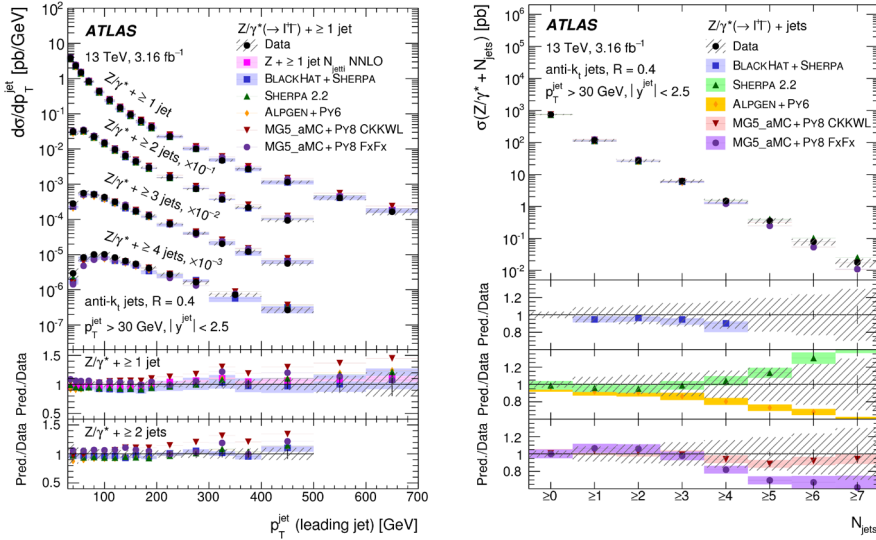


Figure 9. Left: measured cross section as a function of the leading jet p_T for inclusive $Z + \geq 1, 2, 3, 4$ jet events. Right: measured cross section as a function of the inclusive jet multiplicity for $Z + \text{jets}$ events. The data are compared to the predictions from $Z + \geq 1$ jet N_{jetti} NNLO (p_T spectra only), BLACKHAT+SHERPA, SHERPA 2.2, ALPGEN+PY6, MG5_aMC+PY8 CKKWL, and MG5_aMC+PY8 FxFx. The error bars correspond to the statistical uncertainty, and the hatched bands to the data statistical and systematic uncertainties (including luminosity) added in quadrature. Taken from Ref. [5].

good agreement is found within the uncertainties with the generators which use next-to-leading-order matrix elements and the more recent next-to-next-to-leading-order fixed-order predictions.

In particular, leading-order predictions are observed to have a too hard jet p_T spectrum compared to data, for values of jet $p_T > 200$ GeV. Regarding the jet multiplicity observable, the models considered are sensibly underestimating or overestimating the data results for high jet multiplicity (number of jets higher than 4). Both results are shown in Fig. 9.

6 Triple differential Z boson cross section at 8 TeV

The Z boson differential cross section in the lepton decay channel has been measured with 20.2 fb^{-1} 8 TeV data. The results are presented as a function of the invariant mass m_{ll} , the dilepton rapidity $|y_{ll}|$, and the angular variable $\cos\theta^*$, between the outgoing lepton and the incoming quark in the Collins-Soper frame.

The cross sections are used to determine the Z boson forward-backward asymmetry A_{FB} , defined as:

$$A_{FB} = \frac{d^3\sigma(\cos\theta^* > 0) - d^3\sigma(\cos\theta^* < 0)}{d^3\sigma(\cos\theta^* > 0) + d^3\sigma(\cos\theta^* < 0)}, \quad (4)$$

as a function of m_{ll} and $|y_{ll}|$.

The forward-backward asymmetry is found to change sign at the Z boson mass and to increase with $|y_{ll}|$, as expected. A_{FB} values are compatible with 0 for m_{ll} close to Z boson mass, while they are positive (negative) for events with m_{ll} lower (higher) than the Z boson mass.

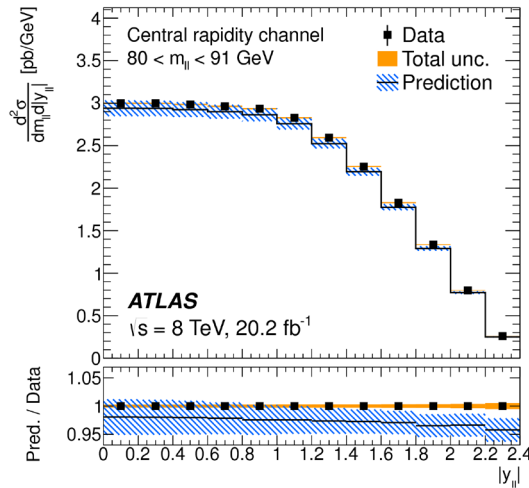


Figure 10. Fiducial cross section as a function of m_{ll} , the dilepton rapidity $|y_{ll}|$ in the invariant mass range close to the Z boson mass. The data are shown as solid markers and the prediction from Powheg is shown as the solid line. The inner error bars represent the data statistical uncertainty and the solid band shows the total experimental uncertainty. The contribution to the uncertainty from the luminosity measurement is excluded. The hatched band represents the statistical and PDF uncertainties in the prediction. Taken from Ref. [6].

The measurements achieve high-precision (1% level, excluding the uncertainty in the integrated luminosity) and are in agreement with predictions, with a slight tendency of the prediction to underestimate the data results, as can be seen in Fig. 10.

7 Drell-Yan lepton angular correlations

The angular correlations between lepton pairs has been measured with 20.3 fb^{-1} 8 TeV data, in the invariant mass region close to Z boson mass. The complete set of angular coefficients A_{0-7} is extracted by polynomial decomposition of the lepton polar θ and azimuthal ϕ angular variables, measured in the Z boson Collins-Soper frame.

Results are compared to several available next-to-next-to-leading-order predictions. Evidence is found for nonzero $A_{5,6,7}$ observables, consistent with expectations. The observable $A_0 - A_2$, built as the difference between A_0 and A_2 , is found to be higher than zero, as expected, when introducing higher order corrections. All the predictions are observed to be a factor of 2 lower than the data results (see Fig. 11).

8 Anti- k_t jet splitting scales

Splitting scales of the jets produced in association with a Z boson, clustered with the anti- k_t algorithm [9], are measured with 20.2 fb^{-1} 8 TeV data. Starting from charged particle tracks as input, jets are clustered according to the minimum distance criteria: minimum distance between the tracks or between the tracks and the beam axes. After the jet clusterization, the splitting scales $\sqrt{d_k}$ are defined as the square root of d_k , where:

$$d_k = \min(d_{ij}, d_{ib}), \quad (5)$$

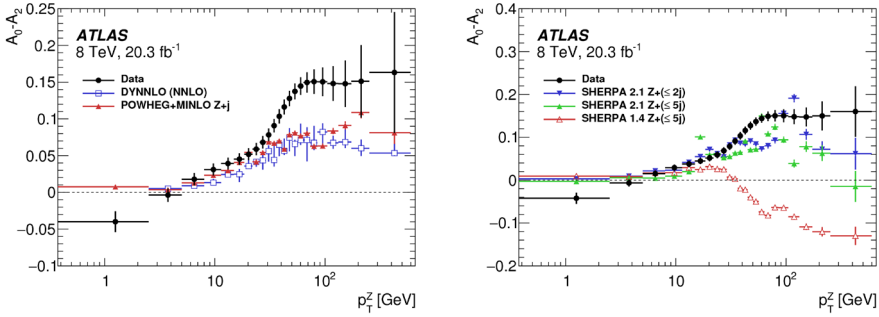


Figure 11. Distributions of the angular coefficients $A_0 - A_2$ as a function of p_T^Z . The results are compared to the DYNNLO and POWHEG MINLO predictions (left) and various SHERPA predictions (right). The error bars for the calculations show the total uncertainty for DYNNLO, but only the statistical uncertainties for POWHEG MINLO and SHERPA. Taken from Ref. [7].

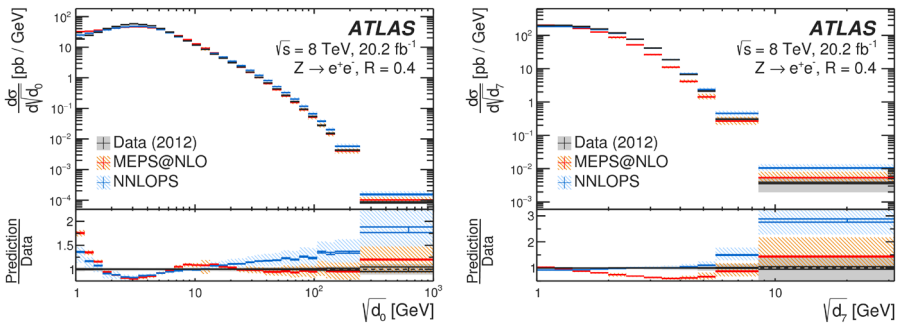


Figure 12. Charged-only distributions for the 0-th (left) and the 7-th (right) splitting scales in the electron channel using the jet-radius parameter $R=0.4$. The size of the error bars reflects the statistical uncertainty, while the combined statistical and systematic uncertainty is indicated by the grey band. Theoretical predictions from SHERPA with NLO multijet merging (MEPS@NLO) and from POWHEG+PYTHIA8 with NNLO matching (NNLOPS) are displayed including error bands for the generator uncertainties. Taken from Ref. [8].

with d_{ij} defined as:

$$d_{ij} = \min(p_{T,i}^2, p_{T,j}^2) \times \frac{\Delta R_{i,j}^2}{R^2}, \quad (6)$$

and d_{ib} as:

$$d_{ib} = p_{T,i}^2. \quad (7)$$

With this definition, the 0-th order splitting scale corresponds to the p_T of the leading jet, while the N -th order of the splitting scale can be interpreted as the distance at which a N jet event can be resolved as a $N + 1$ jet event.

Data results are compared to next- and next-to-next-to-leading-order predictions: significant deviations are found between data and state-of-the-art predictions in various regions of the observables (see Fig. 12). Compatible results are found between the electron and muon channel Z boson decay, and between clusterization performed with the anti- k_T radius parameter equal to 0.4 and to 1.0.

9 Conclusion

High precision ATLAS measurements of vector boson observables have been performed with 7, 8 and 13 TeV data. In several measurements, the experimental precision has been higher than the prediction one: in particular, the uncertainty had been further reduced in the W^+/W^- , W/Z and $t\bar{t}/Z$ cross section ratio measurements, due to the factorization of some systematic uncertainties.

The results have been exploited to improve the *ATLAS-epWZ12* PDF precision and to derive the new version of the ATLAS based PDF, *ATLAS-epWZ16*, having reduced uncertainty compared to the previous version and showing unsuppressed strangeness content.

Several results are found to confirm the needs for higher order corrections. The remaining discrepancies will motivate further work to improve the precision and the modelling of the predictions. ATLAS precision measurements are therefore a powerful mean to improve our understanding of perturbative QCD.

References

- [1] ATLAS Collaboration, JINST **3**, S08003 (2008)
- [2] ATLAS Collaboration, Eur. Phys. J. C **77**, 367 (2017), 1612.03016
- [3] ATLAS Collaboration, Phys. Lett. B **759**, 601 (2016), 1603.09222
- [4] ATLAS Collaboration, JHEP **02**, 117 (2017), 1612.03636
- [5] ATLAS Collaboration, Eur. Phys. J. C **77**, 361 (2017), 1702.05725
- [6] ATLAS Collaboration, Submitted to JHEP (2017), 1710.05167
- [7] ATLAS Collaboration, JHEP **08**, 159 (2016), 1606.00689
- [8] ATLAS Collaboration, JHEP **08**, 026 (2017), 1704.01530
- [9] M. Cacciari, G. P. Salam, and G. Soyez, JHEP **0805**, 063 (2008), 0802.1189v2